Crystal chemistry and IR spectroscopy of Cl- and SO₄-bearing cancrinite-like minerals

P. Ballirano,[1,*] A. Maras,[1] and P.R. Buseck[2]

[1]Dipartimento di Scienze della Terra, Università di Roma "La Sapienza," P.le Aldo Moro 5, I-00185, Rome, Italy
[2]Departments of Geology and Chemistry, Arizona State University, Tempe, Arizona 85287-1404, U.S.A.

ABSTRACT

Cl- and SO₄-bearing cancrinite-like minerals from Italian localities were studied by means of EPMA, X-ray diffraction, and IR spectroscopy to relate their chemical composition, IR data, and structural features. The framework of the cancrinite-like minerals consists of six-membered rings of aluminosilicate tetrahedra stacked along c. Six types of subunits resulting from different stacking sequences can be identified: free channel, cancrinite, sodalite, losod, liottite, and giuseppettite cages. The free channel is possible only with an AB sequence; in fact, the insertion of a C layer interrupts the channel forming the various cages. The occurrence of these structural subunits seems to correspond to the different chemistries of the cancrinite-like minerals, especially their anion content. According to this model, the SO₄ group seems to play a major role. With the exception of giuseppettite, it tends to fill completely the available voids within the frameworks.

INTRODUCTION

The cancrinite-like minerals (Table 1) show interesting structural features such as commensurate and incommensurate superstructures, stacking faults, and a wide range of anion diadochies. They are characterized by the stacking along c of layerlike arrangements of six-membered rings of aluminosilicate tetrahedra. Their ideal formula may be written as $(Na,K,Ca)_{7-8}(Si_6Al_6O_{24})(SO_4,CO_3,S,Cl,F,OH,H_2O)_{3-4}$. Structural refinements indicate an ordered distribution of Si and Al only for the phases characterized by the simple AB sequence. Stacking faults and superstructures have also been observed by electron microscopy (Rinaldi and Wenk 1979) and X-ray precession photography (Brown and Cesbron 1973). Different models of ordering have been proposed to explain the occurrence of superstructures (Grundy and Hassan 1982; Merlino et al. 1991a, 1991b).

Structure determinations have been performed for cancrinite (Pauling 1930; Jarchow 1965; Smolin et al. 1981; Grundy and Hassan 1982), vishnevite (Hassan and Grundy 1984), K-rich vishnevite (Pushcharovskii et al. 1989), hydroxyl-cancrinite (Nadezhina et al. 1991), davyne (Hassan and Grundy 1990; Bonaccorsi et al. 1990, 1992), microsommite (Merlino et al. 1991b), pitiglianoite (Merlino et al. 1991a, 1991b), quadridavyne (Bonaccorsi et al. 1994), bystrite (Pobedimskaya et al. 1991b), and afghanite (Pobedimskaya et al. 1991a). Davyne, microsommite, and quadridavyne can be grouped together in a davyne-type subgroup characterized by the occurrence of . . . Ca-Cl-Ca . . . chains running through the structure, whereas the can-

crinite-type minerals cancrinite, vishnevite, and pitiglianoite are characterized by . . . Na-H₂O-Na . . . chains. All these and the other trigonal and hexagonal minerals with more complex sequences, characterized by the presence of the C layer, can be referred to as cancrinite-like minerals until a more formal definition of the "cancrinite group" of minerals is given by the International Mineralogical Association.

Many difficulties have arisen in structure determinations of the cancrinite-like minerals with complex stacking sequences, especially in locating nonframework anions and cations. In fact, only partial structure refinements for liottite, franzinite, and giuseppettite have been performed, with the goal to determine the correct stacking sequences (Merlino and Mellini 1976; Merlino and Orlandi 1977a, 1977b; Mazzi, personal communication to Merlino; in Merlino 1984). The presence of diadochies and incomplete site occupancies (Mazzi and Tadini 1981) are some possible reasons for the reported problems. Furthermore, the structure refinement of afghanite showed substantial differences between the chemistry derived from the occupancies as determined from X-ray data (especially the anion content) and the analytical chemical data (Pobedimskaya et al. 1991a). No structural data are available for sacrofanite except its possible space group and lattice parameters (Burragato et al. 1980; Ballirano et al. 1995).

Hogarth (1979) suggested the presence of characteristic compositional fields for cancrinite-like minerals; however, the data that were discussed included only cancrinite, vishnevite, davyne, microsommite, and afghanite. Leoni et al. (1979) noted that different anion contents are shown by liottite, afghanite, and franzinite. They were not

---

* Present address: Dipartimento di Scienze della Terra, Università di Pisa, via S. Maria 53, I-56126, Pisa, Italy.

TABLE 1. Structural data for natural cancrinites

Name	References	Space group	Stacking sequence	a (Å)	c (Å)	R^*
Cancrinite	Grundy and Hassan (1982)	$P6_3$	AB	12.59	5.12	0.028
Vishnevite	Hassan and Grundy (1984)	$P6_3$	AB	12.68	5.18	0.037
K-rich vishnevite	Pushcharovskii et al. (1989)	$P6_3$	AB	12.84	5.27	0.063
Hydroxyl-cancrinite	Nadezhina et al. (1991)	$P6_3$	AB	12.74	5.18	0.039
Davyne	Bonaccorsi et al. (1990)	$P6_3$, $P6_3/m$	AB	12.70	5.35	0.049
Microsommite	Merlino et al. (1991b)	$P6_3$	AB	22.16	5.35	**
Pitiglianoite	Merlino et al. (1991a, 1991b)	$P6_3$	AB	22.12	5.22	0.065
Quadridavyne	Bonaccorsi et al. (1994)	$P6_3/m$	AB	25.77	5.37	0.140
Bystrite	Pobedimskaya et al. (1991b)	$P6_3mc$	ABAC	12.86	10.70	0.078
Liottite	Merlino and Mellini (1976)	$P\bar{6}m2$	ABABAC	12.84	16.09	0.140**
Afghanite	Pobedimskaya et al. (1991a)	$P6_3mc$	ABABACAC	12.80	21.40	0.069
Franzinite	Merlino and Orlandi (1977b)	$P\bar{3}m1$, $P3m1$, $P321$	ABCABCBACB	12.88	26.58	†
Giuseppettite	Mazzi pers. com. in Merlino (1984)	$P6_3/mmc$, $P6_3mc$, $P\bar{6}2c$	ABABABACBABABABC	12.85	42.22	0.160**
Sacrofanite	Burragato et al. (1980)	$P6_3/mmc$, $P6_3mc$, $P\bar{6}2c$	†	12.86	74.24	†

$* R = \dfrac{\Sigma (|F_o| - |F_c|)}{\Sigma |F_o|}.$
** Partial structure refinement.
† Unknown data.

able to relate these differences to the cation contents. The same conclusions were subsequently made with respect to giuseppettite (Mazzi and Tadini 1981).

It is difficult to obtain reliable electron microprobe analyses of cancrinite-like minerals because of the presence of H_2O, CO_3 groups, and large amounts of Na. Hence, chemical analyses have been obtained using X-ray fluorescence, atomic absorption, and microanalytical determination of C and H (Merlino and Orlandi 1977a, 1977b; Leoni et al. 1979; Burragato et al. 1980), EPMA (Hogarth 1979; Franceschini and Orlandi 1989; Bonaccorsi et al. 1990; Ballirano et al. 1994, 1995), and wet-chemical analysis (Bariand et al. 1968). The different detection limits, accuracy, and precision of the various methods make a comparison of the compositional data difficult.

The primary goal of this paper is to establish relations among the chemical compositions, the IR spectra, and the structural features of the complex stacking sequences of cancrinite-like minerals.

EXPERIMENTAL PROCEDURES

Twenty samples of Cl- and SO_4-bearing cancrinite-like minerals from different Italian localities were investigated (Table 2). They came partly from private collections and partly from the Mineralogical Museum, University of Rome (MMUR). The specimens 24340 MMUR (franzinite) and 24341 MMUR (giuseppettite) are cotypes of the mineral species, allowing us to make a direct comparison with chemical reference data.

Prior to undertaking the electron microprobe analyses, the samples were embedded in epoxy, and after polishing they were ultrasonically cleaned in spectrophotometric-grade deionized water and heated in an oven at 50 °C for 96 h to eliminate adsorbed H_2O. Compositions were determined using a Cameca SX50 electron microprobe with the following conditions: 10 s counting time (peak), 5 s counting time (background), 10 μm beam diameter, 15 kV excitation voltage, 15 nA specimen current, and

TABLE 2. Samples and cell parameters

Sample	Mineral	Locality	a (Å)	c (Å)
2PAR	davyne-type	M. Somma	12.6711(3)	5.3278(2)
7630 MMUR	davyne-type	M. Somma	12.7565(10)	5.3692(5)
7631 MMUR	davyne-type	M. Somma	12.682(3)	5.321(2)
7644 MMUR	davyne-type	M. Somma	12.8428(16)	5.3760(8)
7648 MMUR	davyne-type	M. Somma	12.6946(7)	5.3364(4)
7651 MMUR	davyne-type	M. Somma	12.7313(11)	5.3511(7)
7672 MMUR	davyne-type	M. Somma	12.7881(8)	5.3509(4)
6a	davyne-type	M. Somma	12.7424(8)	5.3743(4)
22a	davyne-type	M. Somma	12.878(3)	5.370(3)
19106 MMUR	davyne-type	M. Somma	12.882(2)	5.379(2)
1PAR	liottite	Case Collina	12.827(2)	16.116(6)
11PAR	liottite	Case Collina	12.810(1)	16.078(4)
4PAR	afghanite	Case Collina	12.8843(3)	21.4650(25)
9PAR	afghanite	Fosso Attici	12.8532(8)	21.3827(30)
24336 MMUR	afghanite	Case Collina	12.7876(9)	21.4079(24)
7640 MMUR	afghanite	M. Somma	12.803(3)	21.410(8)
5PAR	franzinite	V. Biachella	12.907(1)	26.526(3)
6PAR	franzinite	Fosso Attici	12.902(2)	26.518(5)
24340 MMUR	franzinite	V. Biachella	12.9044(6)	26.5145(18)
24341 MMUR	giuseppettite	V. Biachella	12.8583(12)	42.3059(49)

Note: MMUR refers to samples from the Mineralogical Museum of the University of Rome. PAR and letter "a" refer to samples donated by G.C. Parodi.

TABLE 3. Chemical analyses* and unit formulas, on the basis of 12(Si + Al), for davyne-type minerals

	2PAR	7630	7631	7648	7651	7672	6a	7644	19106	22a
SiO_2	32.87	33.25	33.01	32.92	33.05	32.67	33.04	33.25	32.64	33.10
Al_2O_3	27.32	27.18	27.40	27.34	27.14	26.96	27.35	27.17	27.08	27.24
CaO	11.05	9.63	12.88	12.97	11.07	9.71	10.13	10.28	9.57	9.91
Na_2O	15.29	13.20	13.15	12.82	12.70	11.63	12.39	11.18	10.46	11.71
K_2O	1.12	5.44	2.69	2.87	4.51	7.03	5.81	6.41	8.02	5.40
SO_3	6.48	3.79	1.90	1.35	2.41	4.97	3.91	0.38	0.46	0.72
Cl	6.73	8.93	7.60	7.51	7.75	6.76	8.99	11.47	11.16	10.93
F	0.11	0.08	0.08	0.10	0.05	0.16	0.07	0.03	0.01	0.04
	100.97	101.50	98.71	97.88	98.68	99.89	101.69	100.14	99.40	99.05
O = Cl,F	−1.56	−2.05	−1.75	−1.74	−1.77	−1.59	−2.06	−2.60	−2.52	−2.48
	99.41	99.45	96.96	96.14	96.91	98.30	99.63	97.54	96.88	96.57
CO_2 (estimated)	0.50	0	3.00	3.50	2.00	0.50	0	0	0	0
Total	99.91	99.45	99.96	99.64	98.91	98.80	99.63	97.54	96.88	96.57
Si	6.06	6.11	6.07	6.06	6.10	6.09	6.07	6.11	6.07	6.09
Al	5.94	5.89	5.93	5.94	5.90	5.91	5.93	5.89	5.93	5.91
Ca	2.18	1.90	2.54	2.56	2.19	1.94	2.00	2.03	1.91	1.96
Na	5.50	4.70	4.69	4.58	4.54	4.20	4.42	3.99	3.77	4.18
K	0.27	1.28	0.63	0.67	1.06	1.67	1.36	1.50	1.90	1.27
Σ cations	7.95	7.88	7.86	7.81	7.79	7.81	7.78	7.52	7.58	7.41
SO_4	0.90	0.52	0.26	0.19	0.33	0.69	0.54	0.05	0.06	0.10
Cl	2.10	2.78	2.37	2.35	2.42	2.14	2.80	3.57	3.52	3.41
F	0.06	0.05	0.05	0.06	0.03	0.09	0.04	0.02	0.01	0.02
CO_3 (estimated)	0.12	0	0.75	0.88	0.50	0.12	0	0	0	0
O	24.12	24.01	24.77	24.82	24.48	24.12	23.97	23.98	23.99	23.92
O (recalculated)	24.00		24.02	23.94	23.98	24.00				

* Given in weight percent oxide.

wavelength-dispersive spectrometry (WDS). The following standards were used: wollastonite (Si and Ca), corundum (Al), orthoclase (K), jadeite (Na), barite (S), sylvite (Cl), and fluorophlogopite (F). The raw data were corrected on-line for drift, dead time, and background; matrix corrections were performed with a standard ZAF program. Unit formulas were normalized on the basis of 12(Si + Al).

IR spectra were obtained using a Perkin Elmer 1760 Fourier-transform spectrometer over the range 4000–400 cm^{-1}: 128 scans at a nominal resolution of 4 cm^{-1} were averaged. The instrument was equipped with a CsI beamsplitter and a DTGS detector. The powdered samples were mixed in a 1:100 ratio with 200 mg of KBr to obtain transparent pellets. Measurements were made in air at room temperature.

X-ray data were obtained using both single-crystal (Siemens P4 four-circle automatic diffractometer) and powder diffraction techniques (Seifert MZIV automatic powder diffractometer) depending on the dimensions of the samples. The cell parameters refined from single-crystal data were derived from a least-squares procedure using 36 reflections in the 15–30° 2θ range (graphite monochromatized MoKα radiation). The XRD powder data were collected, in summation step-scan mode, from 3 to 90° 2θ. The instrument was equipped with a diffracted beam, curved crystal graphite monochromator using CuKα radiation. It was operated at 40 kV and 20 mA. The 2θ step size was 0.02°, and the counting time was 10 s/step. External standards NBS675 (fluorophlogopite) and NBS640 (Si) were used to avoid overlapping of the standard and sample peaks. The 2θ error-correction procedure used was a least-squares regression of the Δ2θ (2θ$_{exp}$ − 2θ$_{calc}$) vs. 2θ values of the standards. The least-squares refinement of

lattice parameters was performed using the Appleman and Evans (1973) program, as modified by Benoit (1987).

RESULTS

The samples studied and their cell dimensions are reported in Table 2. Chemical analyses and unit formulas for davyne-type minerals and for liottite, afghanite, franzinite, and giuseppettite are given in Tables 3 and 4, respectively. The infrared spectra of davyne-type minerals, afghanite, liottite, franzinite, and giuseppettite are shown in Figures 1–4.

DISCUSSION

Chemical and IR features

Davyne-type minerals. Only the subcell parameters of davyne-type minerals were determined, without any reference to their superstructure (Table 2). However, on the basis of their extremely large *a* parameters (Bonaccorsi 1993), it seems possible to assign samples 7644 MMUR, 19106 MMUR, and 22a to quadridavyne.

The IR spectra of samples 2PAR, 7631 MMUR, 7648 MMUR, 7651 MMUR, and 7672 MMUR have absorption bands located at about 1500 cm^{-1} resulting from the presence of CO_3 groups (Fig. 1a). The relative intensities of these bands may reflect the different amounts of CO_3 groups per formula unit. From a visual evaluation of the intensities of the absorption bands, it seems that 7631 MMUR, 7648 MMUR, and 7651 MMUR contain the largest amount of CO_3. This observation is consistent with the low total weight percent and relatively large number of framework O atoms calculated for the formulas (Table 3); calculating the weight percent CO_2 necessary to saturate the O excess brings the analysis total close to 100.

TABLE 4. Chemical analyses* and unit formulas on the basis of 12(Si + Al) of liottite, afghanite, franzinite, and giuseppettite samples

	Liottite		Afghanite				Franzinite			Giuseppettite
	1PAR	11PAR	4PAR	9PAR	7640	24336	5PAR	6PAR	24340	24341
SiO$_2$	30.86	31.07	30.59	31.31	31.63	31.58	30.45	31.06	31.07	32.87
Al$_2$O$_3$	26.01	26.10	26.14	26.15	26.66	26.15	26.80	26.74	26.85	27.79
CaO	13.54	13.35	12.02	11.10	11.62	12.94	11.23	10.84	11.08	4.55
Na$_2$O	9.94	10.16	8.82	9.78	11.60	11.45	10.35	10.94	11.03	14.06
K$_2$O	5.11	5.11	8.26	7.57	4.63	3.44	5.81	5.77	5.43	8.12
SO$_3$	11.50	10.67	10.98	10.88	9.56	10.84	13.99	13.60	14.00	9.94
Cl	3.78	4.67	3.31	3.25	4.58	4.39	0.23	0.65	0.20	0.63
F	0.14	0.02	0.56	0.17	0	0.05	0.03	0.05	0.05	0.01
	100.88	101.15	100.68	100.21	100.28	101.06	98.89	99.65	99.71	97.97
O = Cl,F	−0.91	−1.06	−0.98	−0.80	−1.03	−1.01	−0.06	−0.17	−0.07	−0.15
	99.97	100.09	99.70	99.41	99.25	100.05	98.83	99.48	99.64	97.82
CO$_2$ (estimated)	0	0	0	0	0.50	0	0	0	0	0
H$_2$O (estimated)	0	0	0	0.50	0	0	0	0	0	1.50
Total	99.97	100.09	99.70	99.91	99.75	100.05	98.83	99.48	99.64	99.32
Si	6.02	6.03	5.98	6.05	6.02	6.07	5.89	5.96	5.95	6.01
Al	5.98	5.97	6.02	5.95	5.98	5.93	6.11	6.04	6.05	5.99
Ca	2.83	2.78	2.52	2.30	2.37	2.67	2.33	2.23	2.27	0.89
Na	3.76	3.82	3.13	3.66	4.28	4.35	3.88	4.07	4.09	4.99
K	1.27	1.27	2.20	1.87	1.12	0.84	1.43	1.41	1.33	1.89
Σ cations	7.86	7.87	7.85	7.83	7.77	7.83	7.64	7.71	7.69	7.77
SO$_4$	1.68	1.55	1.61	1.58	1.36	1.57	2.03	1.96	2.01	1.36
Cl	1.25	1.54	1.10	1.06	1.48	1.43	0.08	0.21	0.07	0.20
F	0.09	0.01	0.35	0.10	0	0.03	0.02	0.03	0.03	0
CO$_3$ (estimated)	0	0	0	0	0.12	0	0	0	0	0
H$_2$O (estimated)	0	0	0	0.30	0	0	0	0	0	0.90
O	24.01	24.02	23.85	23.93	23.98	24.00	23.87	23.89	23.92	23.89
O recalculated					23.86					

* Given in weight percent oxide.

The weak broad band at 1650 cm^{-1} is due to OH bending of H$_2$O attributed to humidity adsorbed by the sample.

In the 1200–800 cm^{-1} range (Fig. 1b), there are two strong bands at 1120 and 1000 cm^{-1} that have shoulders. There is also a small band at 860 cm^{-1} in the spectra of the samples containing CO$_3$ groups. The 800–400 cm^{-1} range is characterized by a triplet of bands: The first band occurs in the range 690–670 cm^{-1}, and the other bands are at 610 and 560 cm^{-1}, respectively. Two additional bands occur at 450 and 420 cm^{-1}. The position of the first band of the triplet correlates with the a cell parameter (Fig. 5a). According to Ballirano et al. (1991), this band is attributable to an Si-O-Al bending mode; presumably a variation in Si-O-Al angles involved in the expansion of the a parameter causes the observed shift.

The chemical data cover a large compositional range with respect to both anion and cation composition (Table 3). Cl is the prevailing anion, with SO$_4$ subordinate; only small amounts of F were detected. According to the data of Hassan and Grundy (1984) for the cancrinite-vishnevite series, a substitution scheme 2CO$_3$ ⇌ SO$_4$ can be proposed, which is in agreement with the inferred CO$_3$ contents.

There is a correlation between the Cl contents and cell volumes (Fig. 5b). The quadridavyne samples show a completely expanded state that is correlated with the occurrence of the centrosymmetric space group $P6_3/m$ (Bonaccorsi 1993). Cl is particularly effective along the c direction (Fig. 5c). It is evident that the maximum contribution to the expansion of the c cell parameter is reached

with Cl/(Σ anions) equal to about 0.85; values higher than this do not lead to any further increase of the c cell parameter. However, if we include vacancies in the sum of anions, the ratio for quadridavyne is on the order of 0.88.

The relative cation composition is also variable, especially with respect to the K content. There are at least two Ca atoms for the subcell that are located at the center of the six-membered rings forming ... Ca-Cl-Ca ... chains running along c. The remaining cations are located inside the large channel, being disordered between two crystallographic sites, lying nearly at the same c elevation. The site splitting has been attributed to the partial or complete ordering between K and Na,Ca to form favorable M-O (M = K, Na, Ca) bond distances (Bonaccorsi et al. 1990).

The quadridavyne samples are zoned with respect to K/Na, but Na is always the prevailing cation. This zonation is extremely pronounced for sample 19106 MMUR, with K/Na values ranging from 0.25 to 1.

Another correlation involving the K content and the a parameter was observed (Fig. 5d). Only the quadridavyne samples lie off the regression line. This deviation may be due to the compositional zonation of the crystals or the contribution of the volumetric expansion because of the presence of Cl as the only anion.

The quadridavyne samples show an unusually low total weight percent despite the absence of IR absorption bands assignable to H$_2$O or CO$_3$ groups. These samples, furthermore, are not stoichiometric, showing a 0.5 anion and cation deficit. This feature suggests an additional

FIGURE 1. IR spectra of davyne-type minerals. (**a**) Range 1800–1300 cm^{-1}. The two distinct groups of bands in the 1500–1400 cm^{-1} zone are possibly due to CO_3 groups. Samples without bands in this range are not reported for clarity. (**b**) Range 1300–400 cm^{-1}. The samples are arranged, from bottom to top, with increasing frequency of the first band of the triplet located at 700–550 cm^{-1}.

$\longrightarrow$

possible explanation for the superstructure as the result of the ordering of vacancies inside the large channels, according to schemes similar to that proposed for cancrinite (Grundy and Hassan 1982).

Liottite and afghanite. These minerals are characterized, respectively, by ABABAC and ABABACAC stacking sequences. They are grouped together in the present discussion because their SO_4/Cl ratio is close to 1, with a small excess of SO_4 in liottite (Table 4).

IR spectra of liottite and afghanite show features similar to those of the davyne-type minerals. The most striking difference is the number of absorption bands in the range 800–500 cm^{-1}. There are five bands for afghanite and six bands for liottite. The extra band is located at 525 cm^{-1} and allows easy discrimination between the two minerals (Fig. 2c). The correlation between the position of the band at about 680 cm^{-1} and the a parameter is similar to that observed for the davyne-type minerals (Fig. 6a).

Only the IR spectrum of afghanite 9PAR shows OH absorption bands (Fig. 2a). Sample 7640 shows small peaks at about 1500 cm^{-1} (Fig. 2b) attributed to CO_3 groups (cf. sample 7634, Ballirano et al. 1994), whereas the sharp band at 1400 cm^{-1} was also observed in a high-purity sodalite IR spectrum and attributed to an overtone vibration (Zilio and Bagnato 1984). An estimate of the CO_3 content, according to the method explained above, leads to 0.50 wt% CO_2. An additional feature is the presence of significant amounts of F in afghanite 4PAR.

The K/Na ratios vary from 0.20 and 0.70. As in the davyne-type minerals, liottite and afghanite show a linear
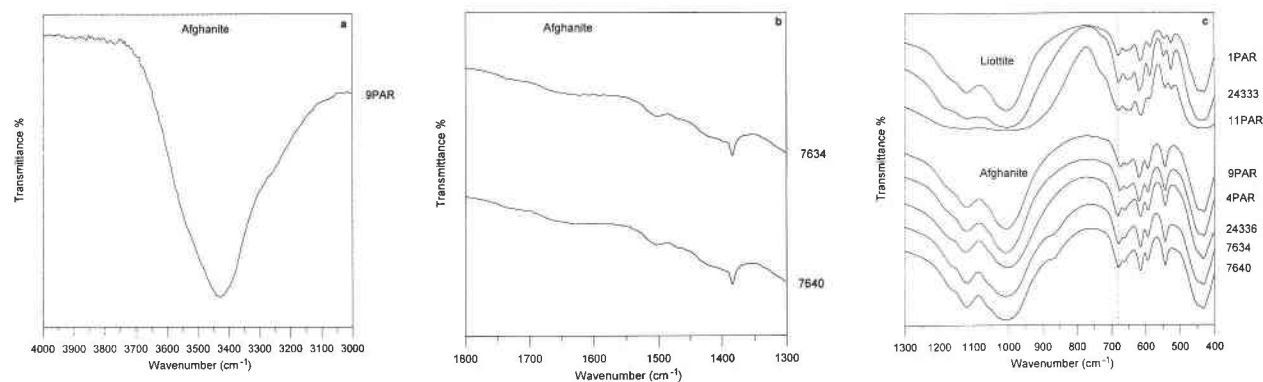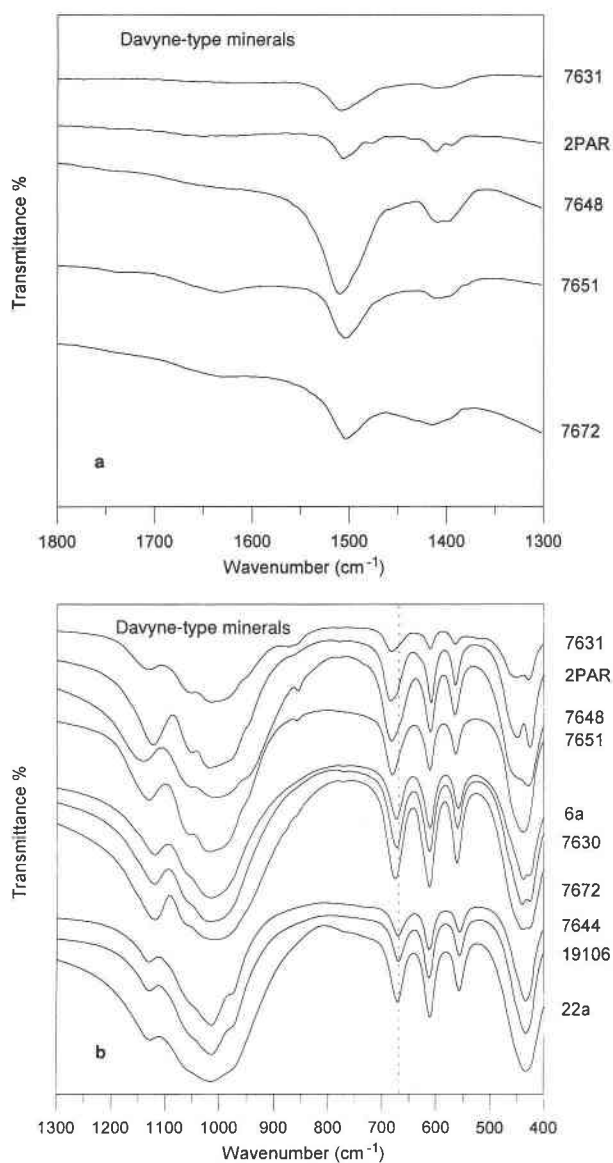
FIGURE 2. IR spectra of afghanite and liottite. (**a**) IR spectrum of afghanite sample 9PAR (from 4000–3000 cm^{-1}). This is the only sample that shows a band that results from the OH stretching vibration of H_2O even after heating at 120 °C for one week. (**b**) Range 1800–1300 cm^{-1}. For clarity, IR spectra of samples that lack features in the range 4000–1300 cm^{-1} are not illustrated. (**c**) Range 1300–400 cm^{-1}. The extra liottite band at 525 cm^{-1} distinguishes between the two mineral phases.
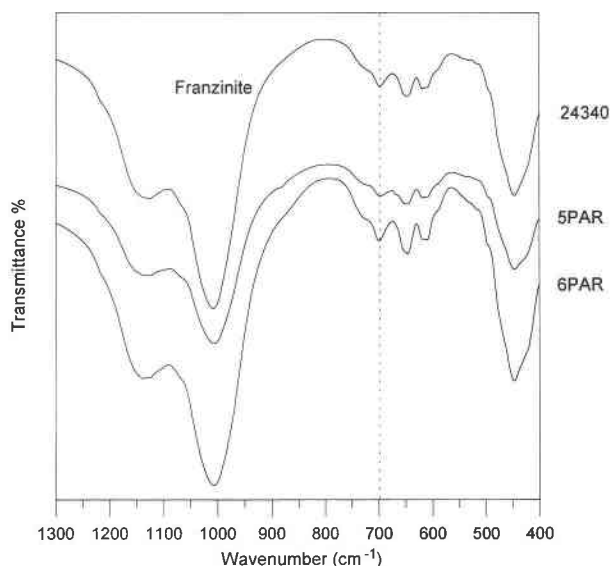
FIGURE 3. IR spectra of franzinite from 1300 to 400 cm^{-1}.

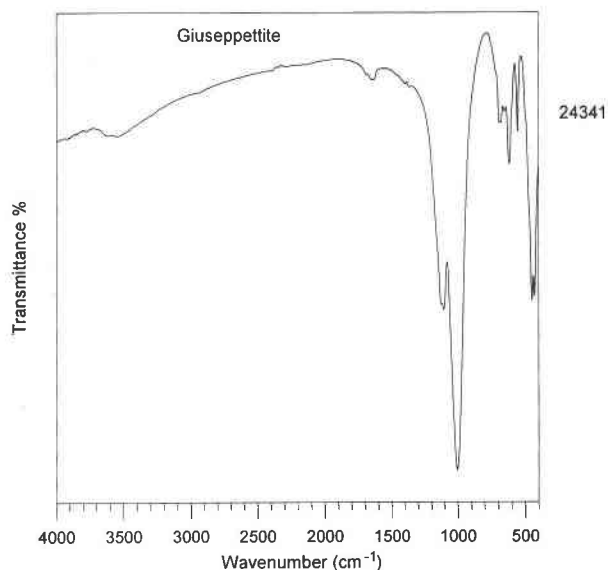**FIGURE 4.** IR spectrum of giuseppettite from 4000 to 400 cm^{-1}.

correlation between the *a* cell parameters and the K content, although the regression coefficients are different (Fig. 6b).

Franzinite and giuseppettite. These minerals are grouped together because they are characterized as having SO_4 as the dominant anion group (Table 4).

Compositionally, all the crystals are homogeneous. There are large discrepancies between our chemical data and the literature data of franzinite, especially with respect to the H_2O and CO_3 content. The IR spectra (Figs. 3 and 4) do not show the presence of CO_3 groups in our samples. However, giuseppettite shows peaks in the OH stretching region; in this regard, franzinite has an analytical total weight percent close to 100, whereas the value is significantly lower for giuseppettite. The IR spectra reflect the complexity of the stacking sequence of these two minerals (franzinite has ten layers with stacking sequence ABCABCBABC; giuseppettite has 16 layers with stacking sequence ABABABACBABABABC), showing a larger number of bands, especially in the range 800–500 cm^{-1}.

The anion composition of franzinite includes two SO_4 groups and minor Cl. The small compositional differences observed among the franzinite samples are reflected in the cell parameters, which are similar. There are significant chemical differences between giuseppettite and the other cancrinite-like minerals (Mazzi and Tadini 1981): The sum of anions is extremely low (1.35 SO_4 and 0.20 Cl), suggesting the presence of significant amounts of H_2O, OH, or both, in agreement with the IR data. Sacrofanite also shows SO_4 as the prevailing anion (Burragato et al. 1980; Ballirano et al. 1995) and for this reason may be added to the group.

3-D structure modeling

We used three-dimensional models to relate chemical features to structural features. This process allowed us to explore the various topologies in search of structural subunits defined by the different frameworks. Six types of such subunits were identified, an uninterrupted channel and five cages: cancrinite, sodalite, losod, liottite, and giuseppettite (Fig. 7). The types and relative positions of the various structural units derived by the different stacking sequences are shown in Figure 8.

The layers of six-membered rings of tetrahedra are stacked along *c* at the following: $1/3, 2/3, z$; $2/3, 1/3, z$; and $0,0,z$. The superposition of such layers gives rise to ordered sequences of structural subunits along these three positions. Two cancrinite cages and a free channel for every subcell are generated by a simple AB stacking sequence, whereas the ABAC stacking sequence (which was found in bystrite) determines a different kind of cage, named a losod cage (Sieber and Meier 1974).

Liottite is characterized by an ABABAC stacking sequence, a topology leading to the so-called liottite cage, which is also typical of afghanite (Podedimskaya et al. 1991a). This cage is formed by the insertion of a C layer, which interrupts the free channel. The liottite framework contains four cancrinite, one losod, and one liottite cage, whereas the afghanite framework (stacking sequence ABABACAC) contains six cancrinite and two liottite cages in the unit cell.

The partial structure determination of franzinite points to an ABCABCBABC stacking sequence (Merlino 1984) leading to six sodalite, two cancrinite, and two losod cages in the unit cell. An interesting feature of franzinite is the presence of sodalite cages originated by the "cubic" ABC part of the stacking sequence.

The framework of giuseppettite, containing the ABABABACBABABABC stacking sequence (Mazzi, personal communication to Merlino; in Merlino 1984), shows one new kind of cage, which we name the giuseppettite cage.
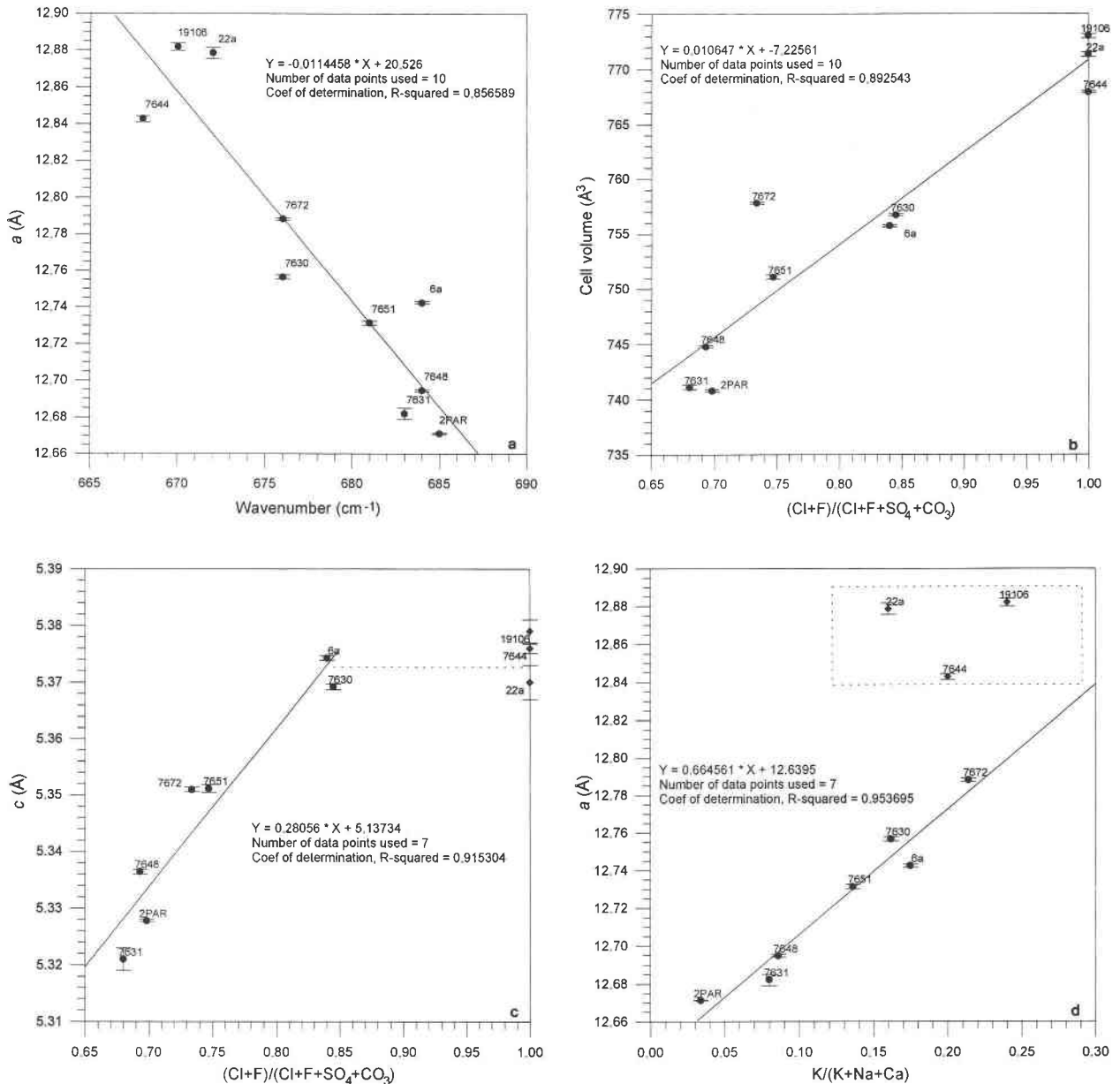
FIGURE 5. (a) Correlation between the a cell dimension and the first band of the triplet located in the range 700–550 cm^{-1} of the davyne-type spectra. (b) Cell volume vs. Cl content of davyne-type minerals. (c) Relationship between the c parameter and the Cl content of davyne-type minerals. The expansion limit is reached at about 0.85. Further increases in Cl content do not seem to expand the c cell parameter. The quadridavyne samples (on the right side of the graph) contain 3.4–3.5 Cl per subcell with respect to the theoretically possible 4.0, leading to a value of about 0.88 when vacancies are included in the calculation. (d) Interdependence of K content and the a cell parameter of davyne-type minerals. Only the quadridavyne samples fall off the regression line, possibly because of inaccurate average bulk-composition calculations, as they are severely zoned.

The unit cell contains ten cancrinite, four sodalite, and two giuseppettite cages.

Geometric constraints

The small cancrinite cage is not able to house SO_4 groups, but it can accommodate both Cl and H_2O. The davyne-type minerals (Bonaccorsi 1993) and cancrinite-vishnevite series (Hassan and Grundy 1984) show [CaCl] and [NaH$_2$O] clusters, respectively. According to Bonaccorsi et al. (1990), the large channels can accommodate a maximum of one SO_4 group, showing extended $2Cl \rightleftharpoons SO_4$ substitution. According to our data, a $2CO_3 \rightleftharpoons SO_4$ substitution may also be hypothesized.

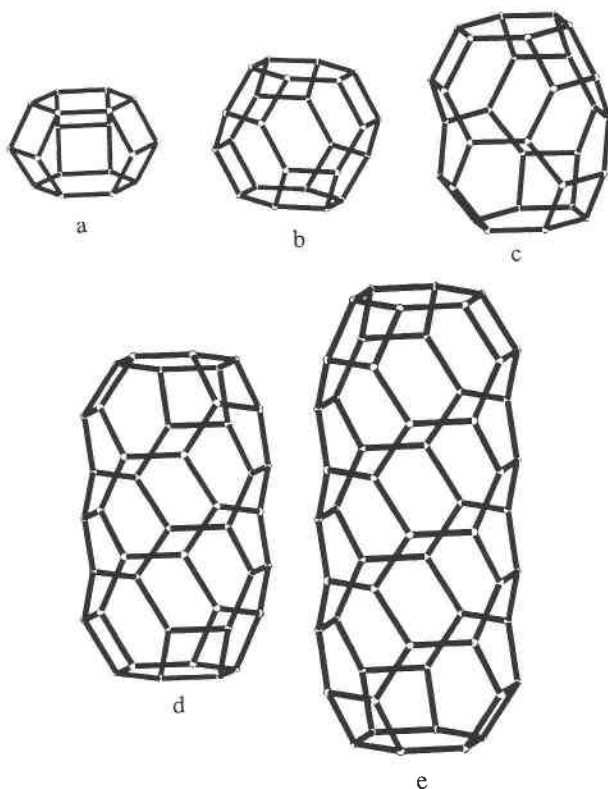Sodalite-type cages occur only in phases with at least
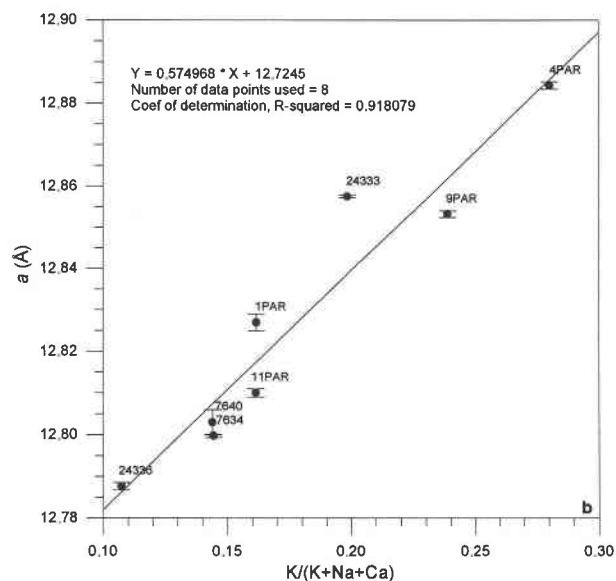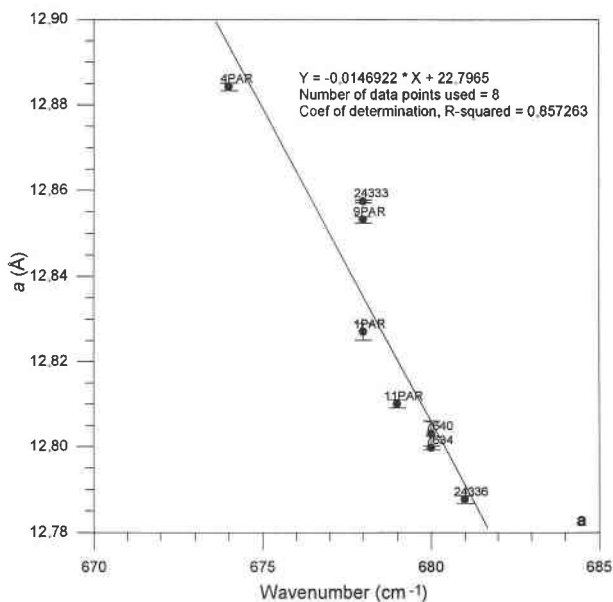
FIGURE 6. (a) Correlation between the *a* cell parameter and the first band of the triplet located in the range 700–550 cm^{-1} of the liottite and afghanite spectra. (b) Plot of K content vs. *a* cell parameter for the same samples.

FIGURE 7. Sketch of (a) cancrinite, (b) sodalite, (c) losod, (d) liottite, and (e) giuseppettite cages. Only T (Si,Al) atoms are shown as small open spheres.
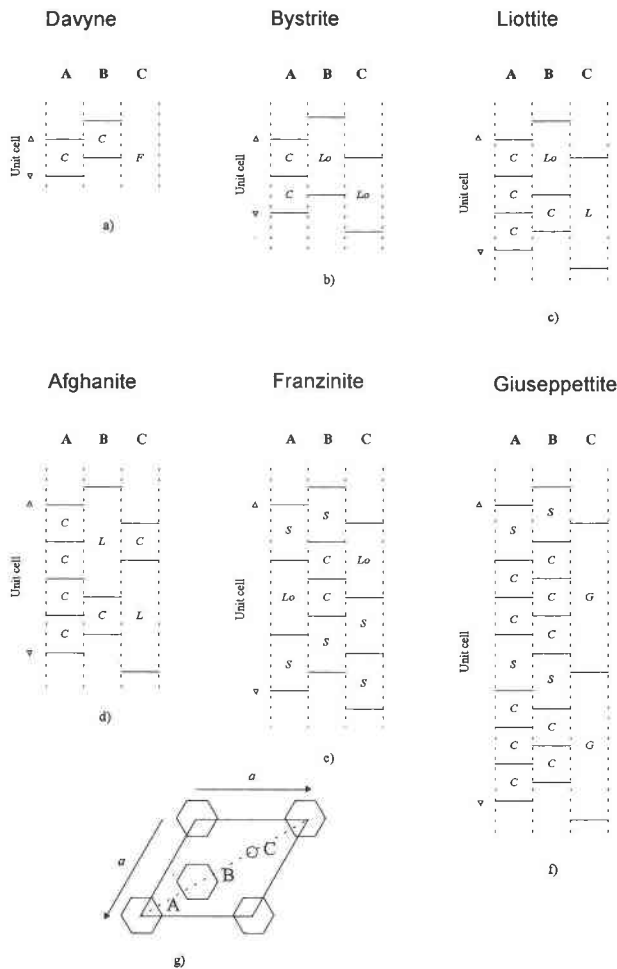
and H_2O as extraframework atoms) does not provide useful information regarding the location of Cl and SO_4.

The liottite cage can host three SO_4 groups (Pobedimskaya et al. 1991a). The cage is base-centered by Ca atoms forming two distinct bond distances of 2.20 and 2.37 Å with the O atoms and 3.49 and 3.63 Å with the S atoms of the sulphate groups. The S-S distances are 4.60 and 4.48 Å, leading to a total height for the liottite cage of 16.2 Å. These bond distances seem to indicate that it is possible to fit two SO_4 groups in a losod cage and four SO_4 groups in the giuseppettite cage.

Crystal-chemical modeling

As a starting point in our discussion we suppose that all cancrinite cages are occupied by Cl atoms and all larger cages by the maximum allowed number of SO_4 groups as derived from the geometrical constraints. Liottite, with its four cancrinite, one losod, and one liottite cage, can contain four Cl and five SO_4 groups. Recalculated on the basis of 12(Si + Al), the formula points to a hypothetical value of 1.33 Cl and 1.67 SO_4, which compares well to the experimental value of 1.44 Cl and 1.65 SO_4 obtained from an average of our data plus those of Ballirano et al. (1995). Afghanite with its ABABACAC stacking sequence, shows six cancrinite and two liottite cages, hous-

ten layers per unit cell. According to Hassan and Buseck (1989), the sodalite cage may host different types of clusters with tetrahedral coordination, as, for example, $(Na_3CaSO_4)^{3+}$, $(Na_4Cl)^{3+}$, and $(Na_4H_2O)^{4+}$.

The only published data for the other structural units refer to losod and liottite cages. The losod cage has been found in both synthetic losod (Sieber and Meier 1974) and natural bystrite (Pobedimskaya et al. 1991b). The very different chemistry involved (losod has Na and H_2O as extraframework atoms; bystrite has Na, K, Ca, S^{2-},

FIGURE 8. Schematic representation of the frameworks of cancrinite-like minerals: (**a**) davyne-type, (**b**) bystrite, (**c**) liottite, (**d**) afghanite, (**e**) franzinite, (**f**) giuseppettite. Solid lines represent six-membered rings of Si,Al tetrahedra. The dotted lines identify the various structural units generated by the different stacking sequences. F = free channel, Lo = losod cage, C = cancrinite cage, L = liottite cage, S = sodalite cage, G = giuseppettite cage. (**g**) Schematic [001] drawing of the framework of an AB-type structure. It is possible to observe the three different positions (A = 0, 0, z; B = 2/3, 1/3, z; C = 1/3, 2/3, z) occupied by the centers of the six-membered rings of Si,Al tetrahedra stacked along c.

ing six Cl and six SO_4 or 1.5 Cl and 1.5 SO_4 on a 12(Si + Al) basis, in agreement with our data and those of Ballirano et al. (1994). Chemical analyses of franzinite give 0.1 Cl and 2 SO_4 on a 12(Si + Al) basis. According to the proposed structural model, we identified six sodalite, two cancrinite, and two losod cages in the franzinite unit cell. Again, assuming the sodalite cages are filled by SO_4 groups, we obtain two Cl and ten SO_4 or 0.4 Cl and two SO_4.

Giuseppettite is characterized by two giuseppettite, ten cancrinite, and four sodalite cages. These subunits can host ten Cl and 12 SO_4, equivalent to 1.25 Cl and 1.5

SO_4 on a 12(Si + Al) basis. Chemical analyses point to two Cl and 11 SO_4, equivalent to 0.25 Cl and 1.37 SO_4, but both IR spectroscopy and HRTEM suggest the presence of large amounts of molecular H_2O. It is not possible to locate exactly the anions inside the subunits because the low SO_4 content is insufficient to fill all the available positions. A possible model would be to consider the two Cl and the 11 SO_4 groups distributed as one Cl and three SO_4 inside the sodalite cages and the remaining eight SO_4 inside the giuseppettite cages. In this way the cancrinite cages may be occupied by one [CaCl] and nine [NaH_2O] clusters. The nine H_2O cluster molecules correspond to 1.5 wt%, in agreement with the low total weight percent obtained from electron microprobe analysis. Confirmation by the direct determination of the H_2O content was prevented by the small amount of available material. The presence of such clusters seems to be confirmed by the high Na content.

As noted, much of the literature data report excessive amounts of CO_3, OH, and H_2O in comparison with our geometrical restraints. In fact, the total number of anions in many chemical formulas considerably exceeds the maximum allowable number of anions per formula unit. The large amount of CO_3 in cancrinite-like minerals with complex stacking sequences (Leoni et al. 1979) could be due to calcite impurity, which is commonly associated with cancrinite. The presence of calcite, however, can be easily detected by IR spectroscopy (significant absorption bands at 1435, 873, and 712 cm^{-1}). Our experiments suggest that the large amount of H_2O may be the result of the strong tendency of all cancrinite-like minerals to adsorb water.

REFERENCES CITED

Appleman, D.E., and Evans, H.T., Jr. (1973) Indexing and least-squares refinement of powder diffraction data. U.S. Department of Commerce, National Technical Information Service Report no. PB216188, 8, 432–435.

Ballirano, P., Burragato, F., and Maras, A. (1991) Sodalite from Vetralla (Roman potassic province) and Bancroft (Ontario, Canada): Observed and simulated IR spectra. Atti dell'Accademia Nazionale dei Lincei. Rendiconti della Classe di Scienze Fisiche, Matematiche e Naturali, serie 9(2), 361–369.

Ballirano, P., Maras, A., Buseck, P.R., Wang, S., and Yates, A.M. (1994) Improved powder X-ray data for cancrinites: I Afghanite. Powder Diffraction, 9(1), 68–73.

——— (1995) Improved powder X-ray data for cancrinites: II. Liottite and sacrofanite. Powder Diffraction, 10(1), 13–19.

Bariand, P., Cesbron, F., and Giraud, R. (1968) Une nouvelle espece minerale: L'afghanite de Sar-e-Sang, Badakhshan, Afghanistan. Com-

parison avec les mineraux du groupe de la cancrinite. Bulletin de la Société Française de Mineralogie et de Cristallographie, 91, 34–42.

Benoit, P.H. (1987) Adaptation to microcomputer of the Appleman-Evans program for indexing and least-squares refinement of powder-diffraction data for unit-cell dimensions. American Mineralogist, 72, 1018–1019.

Bonaccorsi, E. (1993) Feldspathoids belonging to the davyne group: Crystal chemistry, phase transitions and ionic exchanges. Plinius, 9, 16–22.

Bonaccorsi, E., Merlino, S., and Pasero, M. (1990) Davyne: Its structural relationship with cancrinite and vishnevite. Neues Jahrbuch für Mineralogie Monatshefte, H3, 97–112.

——— (1992) Davyne from Zabargad (St. John's) Island: Peculiar chemical and structural features. Acta Vulcanologica, 2, 55–63.

Bonaccorsi, E., Merlino, S., Orlandi, P., Pasero, M., and Vezzalini, G. (1994) Quadridavyne, $[(Na,K)_6Cl_2][Ca_2Cl_2][Si_6Al_6O_{24}]$, a new feldspathoid mineral from Vesuvius area. European Journal of Mineralogy, 6, 481–487.

Brown, W.L., and Cesbron, F. (1973) Sur les surstructures des cancrinites. Comptes Rendues de l'Academie des Sciences Paris, t. 276, serie D, 1–4.

Burragato, F., Parodi, G.C., and Zanazzi, P.F. (1980) Sacrofanite: A new mineral of the cancrinite group. Neues Jahrbuch für Mineralogie Abhandlungen, 140, 102–110.

Franceschini, F., and Orlandi, P. (1989) Ritrovamento della franzinite in una perforazione geotermica dei Sabatini (Lazio). Rendiconti della Società Italiana di Mineralogia e Petrologia, 43, 781–788.

Grundy, H.D., and Hassan, I. (1982) The crystal structure of a carbonate-rich cancrinite. Canadian Mineralogist, 20, 239–251.

Hassan, I., and Grundy, H.D. (1984) The character of the cancrinite-vishnevite solid solution series. Canadian Mineralogist, 22, 333–340.

Hassan, I., and Buseck, P.R. (1989) Incommensurate-modulated structure of nosean, a sodalite-group mineral. American Mineralogist, 74, 394–410.

Hassan, I., and Grundy, H.D. (1990) Structure of davyne and implications for stacking faults. Canadian Mineralogist, 28, 341–349.

Hogarth, D. D. (1979) Afghanite: New occurrences and chemical composition. Canadian Mineralogist, 17, 47–52.

Jarchow, O. (1965) Atomanordnung und Strukturverfeinerung von Cancrinit. Zeitschrift für Kristallographie, 122, 407–422.

Leoni, L., Mellini, M., Merlino, S., and Orlandi, P. (1979) Cancrinite-like minerals: New data and crystal chemical considerations. Rendiconti della Società Italiana di Mineralogia e Petrologia, 35, 713–719.

Mazzi, F., and Tadini, C. (1981) Giuseppettite a new mineral from Sacrofano (Italy) related to the cancrinite group. Neues Jahrbuch für Mineralogie Monatshefte, H3, 103–110.

Merlino, S. (1984) Structures of feldspathoids. In W.L. Brown, Ed., Feldspars and feldspathoids, p. 457–470. Riedel, Dordrecht, the Netherlands.

Merlino, S., and Mellini, M. (1976) Crystal structure of cancrinite-like minerals. Zeolite '76, Proceedings of the International Conference on the occurrence, properties, and utilization of natural zeolites (Tucson). Program and Abstract, 47.

Merlino, S., Mellini, M., Bonaccorsi, E., Pasero, M., Leoni, L., and Orlandi, P. (1991a) Pitiglianoite, a new silicate mineral belonging to the cancrinite group from southern Tuscany. Plinius, 4, 136–137.

——— (1991b) Pitiglianoite, a new feldspathoid from southern Tuscany, Italy: Chemical composition and crystal structure. American Mineralogist, 76, 2003–2008.

Merlino, S., and Orlandi, P. (1977a) Liottite, a new mineral in the cancrinite-davyne group. American Mineralogist, 62, 321–326.

——— (1977b) Franzinite, a new mineral phase from Pitigliano (Italy). Neues Jahrbuch für Mineralogie Monatshefte, 4, 163–167.

Nadezhina, T.N., Rastsvetaeva, R.K., Pobedimskaya, E.A., and Khomyakov, A.P. (1991) Crystal structure of natural hydroxyl-containing cancrinite. Soviet Physics, Crystallography, 36, 325–327.

Pauling, L. (1930) The structure of some sodium and calcium aluminosilicates. Proceedings of the National Academy of Sciences, 16, 453–459.

Pobedimskaya, E.A., Rastsvetaeva, R.K., Terentieva, L.E., and Sapozhnikov, A.N. (1991a) Kristallicheskaya struktura afganita. Doklady Akademii Nauk SSSR, 320, 882–886.

Pobedimskaya, E.A., Terentieva, L.E., Sapozhnikov, A.N., Kasaev, A.A., and Dorochova, G.I. (1991b) Kristallicheskaya struktura bystrita. Doklady Akademii Nauk SSSR, 319, 873–878.

Pushcharovskii, D.Yu., Yamnova, N.A., and Khomyakov, A.P. (1989) Crystal structure of high-potassium vishnevite. Soviet Physics, Crystallography, 34, 37–39.

Rinaldi, R., and Wenk, H.R. (1979) Stacking variations in cancrinite minerals. Acta Crystallographica, A35, 825–828.

Sieber, W., and Meier, W.M. (1974) Formation and properties of losod, a new sodium zeolite. Helvetica Chimica Acta, 57, 1533–1549.

Smolin, Yu.I., Shepelev, Yu.F., Butikova, I.K., and Kobyakov, I.B. (1981) Crystal structure of cancrinite. Soviet Physics, Crystallography, 26, 33–35.

Zilio, S.C., and Bagnato, V.S. (1984) Infrared spectra of natural sodalite. Journal of Chemical Physics, 88, 1373–1376.